

## **Notice of Violation of IEEE Publication Principles**

### **"Design and Performance of an Off-axis Free-form Mirror for a Rear Mounted Augmented-reality Head-up Display System,"**

by Z. An, X. Meng, X. Ji, X. Xu and Y. Liu,  
in IEEE Photonics Journal, Volume: 13, Issue: 1, February 2021

After careful and considered review of the content and authorship of this paper by a duly constituted expert committee, this paper has been found to be in violation of IEEE's Publication Principles.

This paper contains significant portions of original text from the paper cited below. The original text was copied without attribution (including appropriate references to the original author(s) and/or paper title) and without permission.

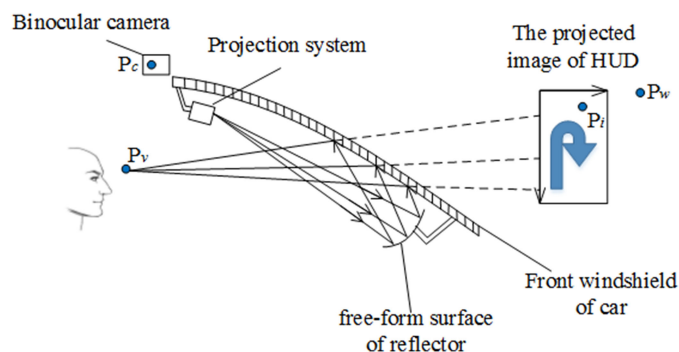
### **"Optical Design of Head-up Displays Using CAD-compatible Freeform Surfaces"**

by P. Ott, P. Pogany,  
in Photonik International, Vol. 1, 2009, pp. 42-45

# Design and Performance of an Off-Axis Free-Form Mirror for a Rear Mounted Augmented-Reality Head-Up Display System

Volume 13, Number 1, February 2021

Zhe An  
Xiangping Meng  
Xiu Ji  
Xiping Xu  
Yang Liu



DOI: 10.1109/JPHOT.2021.3052726

# Design and Performance of an Off-Axis Free-Form Mirror for a Rear Mounted Augmented-Reality Head-Up Display System

Zhe An <sup>1</sup>, Xiangping Meng,<sup>1</sup> Xiu Ji,<sup>1</sup> Xiping Xu,<sup>2</sup> and Yang Liu <sup>2</sup>

<sup>1</sup>School of Electrical and Information Engineering, Changchun Institute of Technology, Changchun 130000, China

<sup>2</sup>School of Optoelectronic Engineering, Changchun University of Science and Technology, Changchun 130022, China

DOI:10.1109/JPHOT.2021.3052726

This work is licensed under a Creative Commons Attribution 4.0 License. For more information, see <https://creativecommons.org/licenses/by/4.0/>

Manuscript received December 14, 2020; revised January 12, 2021; accepted January 15, 2021. Date of publication January 19, 2021; date of current version February 16, 2021. This work was supported by Key scientific research projects of Jilin Provincial Department of Education with Project JJKH20210671KJ. Corresponding author: Xiu Ji (e-mail: jixiu523@163.com).

**Abstract:** A novel optical-transmission rear mounted augmented reality head-up display, which can be used to improve the safety of a driving vehicle, is introduced and investigated in this paper. The proposed system uses an off-axis free-form mirror that serves as asymmetric aberration corrector. The off-axis aberration of the system is analyzed and the mirror is designed to correct both linear astigmatism and spherical aberration. This makes it possible to optimize the whole optical system. We also analyze the relationship between human eyes and the virtual image to obtain a registration matrix. The experimental results show that the size of the virtual image is 11 inches, the imaging distance is 2.8 meters, and the area of the eye box is  $140 \times 60 \text{ mm}^2$ . The novel system makes it possible to fuse the virtual image with the real-life scene to improve driver safety.

**Index Terms:** Optical transmission system, off-axis reflector, freeform surface, AR-HUD, virtual-real registration.

## 1. Introduction

A vehicle drivers' dashboard is typically located close and below the driver's line of sight, while the (real-life) road scene is located directly ahead of the driver's line of sight. To observe both the dashboard and the road scene, the driver needs to divert his line of sight. Because the dashboard is close to the driver's eyes, while the scene is located far away from driver, the driver needs to change focus when switching between the two. In addition, there is a substantial difference in quality and intensity between the light inside and outside, which requires time for adaption. In other words, it is practically impossible for drivers to watch the road without visual distraction with conventional dashboards. At typical vehicle speeds, especially when driving at night, a short visual distraction can cause a major traffic accident. Conventional dashboards are struggling to communicate today's large and increasing amount of information safely and comfortable to the driver. Augmented reality (AR) technology [1]–[5] is a possible solution to project larger amounts of information safely to

the driver. This frees the driver from viewing a complicated instrument panel, and reduces the possibility of cognitive overload, which can lead to accidents.

Many modern automobiles are now equipped with an augmented-reality head-up display (AR-HUD)[6]–[10] to reduce distraction of the driver. Head-up display systems can be categorized as follows:

1) Combiner AR-HUD-based [11]–[14]: most of these optical systems have transparent plates to display images and visually combine them with the road scene. Unfortunately, in case of a collision, these plates also represent an additional safety hazard for the driver. One way to avoid this added risk factor is to use the windshield to display the projected information. The problem with windshields is that they typically have an irregular and asymmetric surface that requires some mechanism to correct the distortion of projected symbols.

2) Holographic AR-HUD-based[15]–[18]: A holographic optical element can display a highly reflective narrow-band symbol image, while allowing high-transmittance of light from outside. This way it is possible to improve the display brightness of the image substantially. The symbol image transmitted by the image-source passes through a relay system before it passes through a plane mirror to form an intermediate image. In the center of the system is a holographic combination glass, designed to display the information directly to the eyes. Using this structure, both volume and weight of the system can be reduced. However, the structure still needs to be attached to the windshield glass, which adds complexity and increases cost. Because the holographic optical elements(HOEs) are transparent and thin, K. Bang *et al.* [19] analyzed the influence of the surface curvature of the holographic optical elements on its optical characteristics, designed an optimal curvature method to reduce aberrations, and bends the holographic optical elements and applied it to head-up display.

3) Fresnel lens AR-HUD-based [20]–[22]: The Fresnel lens system has a simple structure, a small volume, and is light-weight. In addition, the Fresnel lens can also correct the aberration caused by the windscreen. The axial aberration of the system, however, is very large.

Wang researched and designed the optical structure of the vehicle-mounted head-up display, and elaborated on the relationship between the various system parameters of head-up display and the determination method [23]. By analyzing actual needs, draw up various system parameters, and use reflective optical structures to integrate well with vehicles. Through the digital light processing (DLP) projection lens imaging, a miniature projection system and a reflective optical system are designed to form a sufficiently large field of view, rich and clear image on the windshield, and the simulation results are analyzed. Zhao took special vehicle drivers as the test object, and established a head-up display brightness adjustment model for the night vision vehicle head-up display brightness display characteristics [24]. The adaptability of the driver group to the display brightness of the night vision vehicle head-up display in the dark environment at night was discussed, and the night vision vehicle head-up display driver dimming experiment was carried out. According to the experimental data, the driver's head-up display brightness curve model in the dark environment at night is established, which provides the basis for the ergonomic optimization design of the night vision vehicle head-up display. Chen proposed a digital light processing (DLP) based head-up display miniature projection display optical system [25]. The compound eye lens is used to homogenize the light emitting diode (LED) light source, the projection lens is used for imaging. The volume is small, and the imaging quality meets the requirements of use. In order to realize the control display of the parallax, Luo Gu *et al.* [26] proposed an optimization strategy for the forward ray tracing mode that directly controls the binocular parallax. The eye box size of the proposed system is  $120 \text{ mm} * 80 \text{ mm}^2$ , and the parallax of the eyes is evaluated and corrected. KUM-HO *et al.* [27] designed a confocal off-axis optical system by analyzing the off-axis aberration of head-up display. This method can easily balance the residual aberration. Qin *et al.* [28] used a picture generation units(PGU) and a curved mirror to perform imaging separately to obtain two focal planes, and optimized the optical design and mechanical structure. Kim *et al.* [29] used a cylindrical lens as an asymmetric aberration corrector to obtain a corrected linear astigmatism and spherical aberration optical system. The distance of the virtual image is 2 meters, the display size is 10 inches, and the eye box area is

130×50mm<sup>2</sup>. Wei *et al.* [30] placed the image source, plane mirror, and free-form surface mirror on the same horizontal plane, and designed structural constraints and optimization strategies. No matter where the pupil is located in the rectangular eye socket, the human eye can observe the virtual image.

The current research is mainly aimed at a certain type of windshield surface. The ideal augmented-reality head-up display must realize the real-time fusion of virtual information and real scenes, and ensure the realism of the fusion of virtual and real, and there are certain requirements in the optical design. Most of the current methods are aimed at a single face, but if it is a different model, the face shape of the windshield will change to a certain extent, which will lead to drift in the process of virtual reality. As for the rear mounted augmented-reality head-up display system, the face of the windshield will change according to different car models. Therefore, in order to solve this problem, this article has solved it. When designing, first obtain the windshield surface data of several kinds of cars, and then use the surface fitting method to obtain a new surface. Use this surface to perform the optical system design. The following two methods are used to compensate for the fitting errors that appear in the fitting process. The first method is to divide the surface into blocks and obtain the fitting results respectively. Since the virtual and real registration can obtain the relationship between the virtual image and the human eye in the actual state, the error can be compensated for the second time during the virtual and real registration. So that the augmented-reality head-up display system can adapt to most models. To solve the above problems, a reflective off-axis optical system was used as optical display-component for the system. In addition, a free-form reflector was designed to correct any image distortion caused by the windshield. We then analyzed the relation between the human eye, the optical system (virtual image) and the real-life scene. We found that the combination of virtual image with real-life scene improves driving safety significantly.

## 2. Design

### 2.1 Principle of an AR-HUD

The augmented-reality head-up display system consists of a tracking camera, projection module, a freeform off-axis reflector system, and a host. First, the road scene is obtained from the tracking camera. Then the road scene is identified by the host computer, and the virtual real registration matrix between different scene frames is calculated. After calculating the location of the virtual image, the host sends information to the projection module via data wire. The projection module projects information onto a specially designed free-form reflector. The information is reflected on the windshield through the reflector, such that the driver can see the virtual image in front of him/her. The working principle is shown in Fig. 1.

### 2.2 Optical Design of the AR-HUD System

Due to limitations in the available optical materials, it is difficult to combine both large aperture and low weight of the refraction system. If the optical imaging system uses a total reflector it becomes possible to reduce weight. This is because the mirror is limited by material, and no chromatic aberration at all. It has high transmittance and is widely used in the design of space optical system. A traditional total reflection system can use only a few parameters to tune aberration, which makes it difficult to achieve a large field of view and small F number at the same time. The field of view of a coaxial reflection system is small, and obscurity in the center can reduce image quality substantially. On the other hand, there is no central occlusion in an off-axis reflector system. This means it becomes possible to optimize many variables and improve the field of view, which increases the imaging quality of the overall system. Therefore, we used a reflective off-axis system. Unlike axisymmetric optical systems, off-axis systems contain partial tilting and eccentric optical elements. The aberration of an optical system is a vector. For a system that

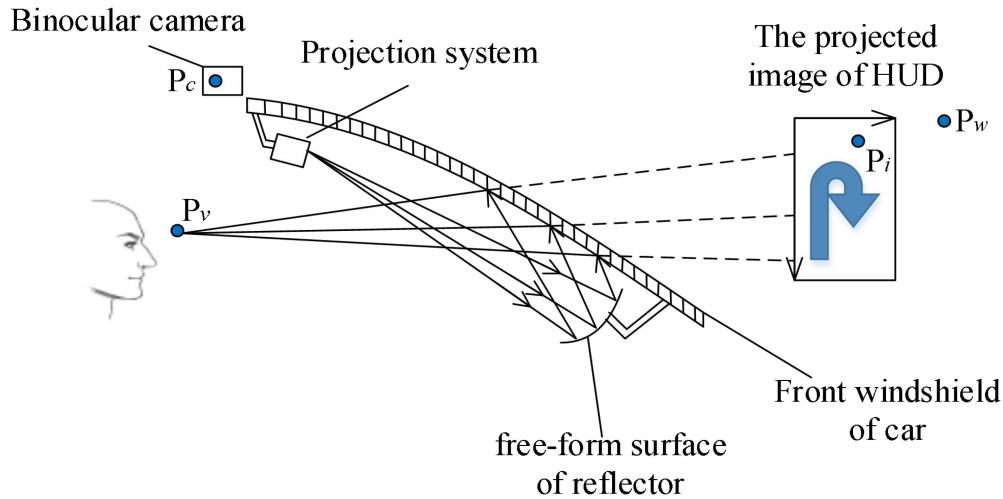


Fig. 1. Schematic diagram of the AR-HUD.

rotates symmetrically about the optical axis, polar coordinates are useful to represent the three order wavefront aberration of the  $i$ th plane of an optical system.

$$W(H, r, r \cos \varphi) = W_{040i}r^4 + W_{131i}Hr^3 \cos \varphi + W_{222i}H^2r^2 \cos^2 \varphi + W_{220i}H^2r^2 + W_{311i}H^3r \cos \varphi \quad (1)$$

Here,  $H$  represents the normalized point coordinates of a coaxial optical system; the distance between the pupil and the normalized optical system is  $r$ ,  $\varphi$  is the azimuth coordinate of the pupil for a given meridian plane. The wavefront aberration of an optical system is the sum of the aberration produced by all image planes in the system.

$$W = \sum W_i \quad (2)$$

The vector form of formula (1) is:

$$W_i = W_{040i}(r \cdot r)^2 + W_{131i}(H \cdot r)(r \cdot r) + W_{222i}(H \cdot r)^2 + W_{220i}(H \cdot H)(r \cdot r) + W_{311i}(H \cdot H)(H \cdot r) \quad (3)$$

It is assumed that the system revolves around the optical axis.  $s_i$  is the deviation from the center of the aberration field,  $W_i$ , to the center of the aberration field of the optical system. After replacing  $H$  with  $H - s_i$ , we obtain an expression for the three level wavefront aberration vector in the  $i$ th plane.

$$W_i = W_{040i}(r \cdot r)^2 + W_{131i}[(H - s_i) \cdot r](r \cdot r) + W_{222i}[(H - s_i) \cdot r]^2 + W_{220i}[(H - s_i) \cdot (H - s_i)](r \cdot r) + W_{311i}[(H - s_i) \cdot (H - s_i)][(H - s_i) \cdot r] \quad (4)$$

The wavefront aberration of the system can be formulated as:

$$W = \sum W_i = \sum W_{040i}(r \cdot r)^2 + \sum W_{131i}[(H - s_i) \cdot r](r \cdot r) + \sum W_{222i}[(H - s_i) \cdot r]^2 + \sum W_{220i}[(H - s_i) \cdot (H - s_i)](r \cdot r) + \sum W_{311i}[(H - s_i) \cdot (H - s_i)][(H - s_i) \cdot r] \quad (5)$$

A small manufacturing error in the production process can have a strong effect on the image quality of the head-up display. Even if ideal manufacturing precision could be achieved, and there is no error in the installation of the windshield of the flat-view display system. However, during the day or night, with a large range of observation of pupil to people, the effect of system aberration on the quality of the virtual images is not clear because there are many types of aberrations



such as position chromatic aberration, lateral chromatic aberration, spherical aberration, comatic aberration, and the effect of field curvature. While these aberrations do not directly depend on the manufacturing tolerances of the windshield or the range of the driver's head movements, they still affect the image quality. This is particularly important for the reflective structure of a flat-view optical system because of the color difference and refraction of the system. In addition, because there is no lens in the reflected vehicle flat-view display system, a system using a reflective structure does not have any chromatic aberration. However, the degree of spherical aberration is determined by spherical lenses and spherical reflectors. These elements are usually used for astronomy and photography. Because the complications to manufacture spherical elements are fewer than for aspherical surfaces, production costs are lower. A combination of concave convex spherical or aspherical lens can be used to eliminate spherical aberration. Because the vehicle-mounted head-up display system investigated in this paper is reflective, the aberration is corrected for using a curved reflector. This means the manufacturing accuracy of the head-up display mirror must be controlled strictly.

Importantly, the distortion of an augmented-reality head-up display system also changes the shape of the image, which makes the information harder to read. The larger the distortion the higher the risk for an accident. In fact, people's eyes are usually located at the edge of the pupil range or near the edge of the eye, and the distortion in this position is especially easy to attract people's attention. The surface shape of the reflector is designed, and the free-form surface is designed to meet the design requirements. The eyebox is a space, where the eyes can see the visual effect of the mobile AR-HUD. Larger eye-movement requires more luminous flux. Small eye movements limit the free movement of human eye, which makes it easy to lose sight of the information. Reasonable eye-movement refers to the balance between the two. Considering the above factors, the following parameters for the system were selected: (1) system resolution:  $640 * 480$ ; (2) horizontal field angle:  $\geq 8^\circ$ ; (3) vertical field angle:  $\geq 5^\circ$ ; (4) eye box:  $140 * 60 \text{ mm}^2$ ; (5) projection size: 11 inches.

This system uses the windshield to display the projected image. Unfortunately, the reflection ratio of a typical front windshield is relatively low. While a sun-filtering film can be attached to the front of the windshield to improve the reflection ratio, it can still be difficult to see the projected image in strong sunlight. The situation can be improved by increasing the brightness of the light source. However, a bright light source may cause problems with heat dissipation. According to automotive industry standards, devices located in the dashboard of a car should work normally for temperatures up to  $120^\circ\text{C}$ . Therefore, effective cooling methods are required, and both high brightness and homogenization are key characteristics. In addition, the output-beam quality of the light source is higher. At the same time, we should consider the thermal stability, vibration resistance and operating life of the light source. For this paper, a high-power LED array was used as a light source. A lens array was placed in front of the LED array to generate the light beam, which uniformly illuminates the Liquid Crystal Display (LCD) panel. The working temperature of a high-power LED is typically quite high, and the temperature in a car may reach about  $50^\circ\text{C}$  in summer. To ensure normal operation of the system, a heat dissipation device was installed after installation of the light source.

### 2.3 Virtual-Real Registration Method of AR-HUD System

In the AR-HUD system, virtual images need to be combined with the real scene, so that the driver can observe the virtual information and road scene together. Next, we try to obtain the relationship between driver, optical system, and road scene. To determine how the external world is mapped to the user's field of view, so that the display can realistic appropriate images. After designing the optical display system, we need to obtain the relationship among human eyes, display device, real scene and virtual image display plane. The coordinate relationship is shown in Fig. 2. In Fig. 2,  $w$  represents the world coordinate system, and  $c$  is the camera coordinate system.  $v$  represents the virtual camera coordinate system, which is composed of the optical system and the human eye.  $l$  is the virtual plane coordinate system. If we let  $P_w = (x, y, z)$  represent any point on the object,  $P_c$  is the point that corresponds to  $P_w$  below the tracking camera.  $P_v$  is the corresponding point

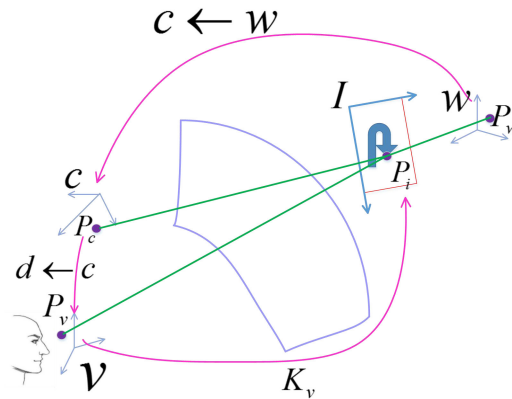


Fig. 2. The coordinate relationship of AR-HUD.

in the human eye coordinate system. The human eye sees the virtual image through the optical system. Both, eye and optical system, constitute the combined imaging system, which is defined as the virtual phase machine coordinate system.  $P_i$  is a pixel point within a virtual image plane. The amount of coordinate change is represented by the rotation variable  $r$  and the translation variable  $t$ . By establishing the relationship between the above points, we can get the registration matrix of virtual and real information, and determine the location of virtual information projection.

The relationship between these can be expressed as:

$$P_i = K_v^{3 \times 4} \begin{pmatrix} r^{3 \times 3} & t^{3 \times 1} \\ v \leftarrow c & v \leftarrow c \\ 0 & 1 \end{pmatrix} \begin{pmatrix} r^{3 \times 3} & t^{3 \times 1} \\ c \leftarrow w & c \leftarrow w \\ 0 & 1 \end{pmatrix} P_w \quad (6)$$

Where  $K_v$  is the virtual camera control,  $r$  and  $t$  represent, respectively, the translation and rotation matrix of the camera.

In solution (6), the depth  $d$  for the object pixel in the image was determined using monocular depth estimation [31]. Assuming the coordinates of a pixel point on the road-scene object obtained using image recognition are  $(u, v, d)$ , the equation that converts this point into the space point  $p_w$  is:

$$\begin{cases} x = \frac{z}{f_x}(u - c_x) \\ y = \frac{z}{f_y}(v - c_y) \\ z = \frac{d}{s} \end{cases} \quad (7)$$

Where  $s$  is the depth scaling factor, and  $f_x$ ,  $f_y$ ,  $c_x$ ,  $c_y$  are internal references of the camera. We use the result from (2) as inputs for formula (1). Using the matrix solution, the transformation matrix of the spatial coordinates  $p_w$  relative to the corresponding point  $p_i$  on the virtual plane can be obtained, which is defined as the initial transformation matrix  $A$ . When a new frame is generated, the posture change of the camera causes a change for the virtual reality registration matrix. In this moment, the feature points of the input images between the two key frames are extracted, and the feature points of the two pictures are matched. Then, the two dimensional points are converted to three dimensional points using the depth data of the points, considering  $p = \{p_1, \dots, p_m\}$  and  $p' = \{p'_1, \dots, p'_m\}$ . The matching space points are transformed using  $R$  and  $T$  to satisfy the following relation:

$$p_i = R p'_i + T \quad (8)$$

One problem is the camera pose estimation, i.e., to estimate the upper form of  $R$  and  $T$ . To solve this problem, we use the Iterative Closest Point (ICP) method [32]:

$$e_i = p_i - (R p'_i + T) \quad (9)$$



The camera pose matrix  $R$  and  $T$  can be solved using the least square relation:

$$\min J = \frac{1}{2} \sum_{i=1}^n \|e_i\|_2^2 = \frac{1}{2} \sum_{i=1}^n \|[p_i - (Rp'_i + T)]\|_2^2 \quad (10)$$

The camera pose estimation not only considers the constraint relation between feature points, but also increases the constraint relationship between objects of the same category. The registration matrices  $R$  and  $T$  for the relative initial location of the camera are  $B$ . The virtual real registration matrix  $T_v$  can be formulated using the initial registration matrix  $A$  and  $B$  synthesis matrix:

$$T_v = A \cdot B \quad (11)$$

This way the virtual reality registration matrix is obtained, and the virtual image can be superimposed on the road scene, so that the driver can see a fusion of the virtual and real images.

### 3. Results and Analysis of System Design

#### 3.1 AR-HUD Optical Design Process and Results

The free-form surface shape is designed according to the surface shape of the windshield. Traditional head-up display used flat mirrors for reflection when imaging. However, when the light is reflected on the windshield through the flat reflector, the curvature of the windshield will cause imaging distortion. The curvature of the windshield is also different for different models of cars. Therefore, when modeling the three-dimensional surface of the windshield, the windshield surface of different manufacturers should be considered for modeling, and the corresponding mirror surface should be designed. This design wants to obtain a larger field of view and a longer virtual image imaging distance, which will lead to an increase in the aperture of light. At the same time, the magnification of the system will increase accordingly. When designing a free-form surface mirror, the degree of curvature of the mirror will also increase. The imaging effect of a mirror with a large curvature in the edge field of view is not good enough. So it is necessary to solve this problem by optimizing the optical system. Therefore, when modeling the windshield, first obtain the windshield surface shape of different manufacturers, and take some points in the display area of different windshields, and fit these points to a surface fitting method. So we get a new windshield surface. When designed a free-form surface mirror, the main characterization function of a polynomial free-form surface is based on a conical surface plus a coordinate-related polynomial group characterization function. In the design, an XY polynomial free-form surface is used to optimize the design. The design function is as follows:

$$z = \frac{c_j r_j^2}{1 + \sqrt{1 - (1 + k_j) c_j^2 r_j^2}} + \sum_{i=1}^t C_i x^m y^n \quad (12)$$

Where  $z$  is the vector height of the free-form surface,  $c$  is the curvature at the vertex,  $r$  is the radial length,  $k$  is the conic coefficient, and  $C_i$  is the polynomial coefficient. In order to ensure accuracy, the surfaces are optimized separately. In the design, according to the changing trend of the surface shape, the new windshield surface is divided into four parts, which are represented by  $j = 1, 2, 3, 4$ . We select the highest order of  $x$ ,  $y$  as  $m + n = 4$  to get adequate surface accuracy in this system. When setting optimization variables, first set the radius of curvature as a variable, then consider adding the diaphragm position as a variable, and then determine the distance between the free-form surface mirror and the windshield. The main optical system aberration correction is for spherical aberration, comatic aberration, astigmatism, field curvature, and distortion. While tilt and eccentricity of the components do not affect spherical aberration, aberrations of higher power affect all lower power aberrations such as the eccentric aberration, astigmatism, field curvature, and distortion. Similarly, eccentric astigmatism affects both field of view and distortion. Because a reflective optical system can only use a few surfaces, aspheric aberration correction is often used. An off-axis reflective optical system can use a free-form surface to correct aberration. This

TABLE 1  
The Lens Data of AR-HUD System

	Surface type	radius	material	distance
Eyes	Aperture standard surface	Inf.	-	959.852
Virtual image	Object standard surface	Inf.	-	-2800.000
windshield	Image standard surface	Inf.	minute surface	-240.525
Freeform mirror	XY polynomial surface	28.375	minute surface	128.998
Image source	XY polynomial surface	-	minute surface	-

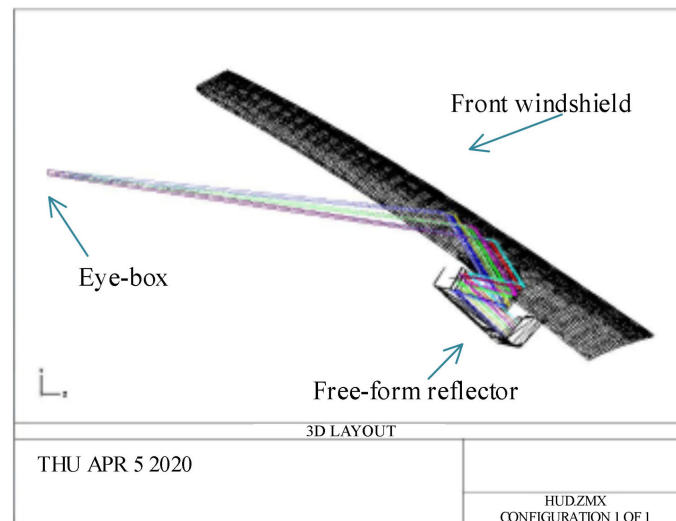


Fig. 3. Final design of the off-axis reflector free-form AR-HUD optical system.

paper uses the special properties of an XY polynomial free-form surface, which can correct off-axis aberration well. In other words, we can now ensure that the images are clearly visible on the windshield. Tabel 1 is the lens data of system.

For the system, we use zemax software for optical design. We set the horizontal angle of view of the optical system greater than, or equal to,  $8^\circ$ , and the vertical field of view is greater than, or equal to,  $5^\circ$ . The eye movement range is  $140\text{mm} \times 60\text{mm}^2$ , which is consistent with the possible head movement range of the driver (during driving). The virtual image size is 11 inches. The size of the virtual image was carefully chosen such that it will not cause visual fatigue and it can show information at the front of the line of sight. The final off-axis reflective design using a freeform surface is shown in Fig. 3. In addition, we built a test system in the laboratory, as shown in Fig. 4.

After optimization of the optical system, we can assess the design considering optimized aberration and performance analysis and the design objects. In the following we provide the analysis and discussion of the designed head-up system. In this design, considering the visual characteristics of the human eye, we analyze the modulation transfer function (MTF) change for the spatial frequency of 6lp/mm. The modulation transfer function curve is shown in Fig. 5.

MTF is the evaluation method of optical system in wave optics. In general, when designing HUD, the higher the line position of MTF is, the better. The slower the downward trend is, the better. If the modulation transfer function value is greater than 0.9, the design result is very well, 0.7–0.9 is better, and 0.4–0.7 indicates that the imaging requirements are basically met. Take the space frequency corresponding to the size of a pixel on the LCD display panel, and the space frequency MTF value under the target image source size should be greater than 0.4, which basically meets

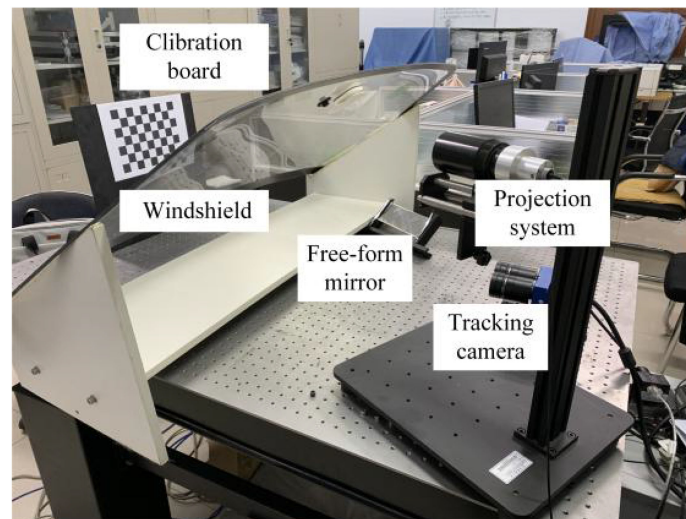


Fig. 4. The experimental system of AR-HUD.

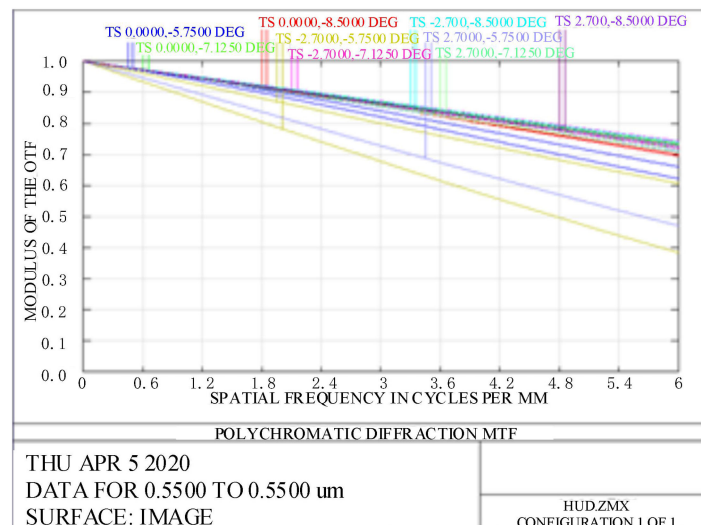


Fig. 5. MTF curve for AR-HUD optical system.

the design requirements. The Fig. 5 shows that the MTF of the system is greater than 0.4 when the spatial frequency is 6lp / mm, so the designed system can basically meet the display requirements of AR-HUD. A Spot chart for the system is shown in Fig. 6. The spot RMS radius is smaller than the radius of the airy pattern. The aberrations are sufficiently balanced in all fields. As a result, the mean square spot size of most fields is below 25  $\mu\text{m}$ , and the imaging quality for each field is sufficient. This means, not only the performance specifications were met but also space is left for processing and assembly of the system.

The distortion curve of the system is shown in Fig. 7. The distortion near the field of view in the system center is below 2%, and the maximum distortion of the field of view is below 4%. While there are still some distortions, the small aberrations can hardly be seen. Overall, the novel system shows good imaging properties.

The virtual image produced by the computer can be fused into the real environment using the virtual-real registration method described in this paper. In order to represent the design results,

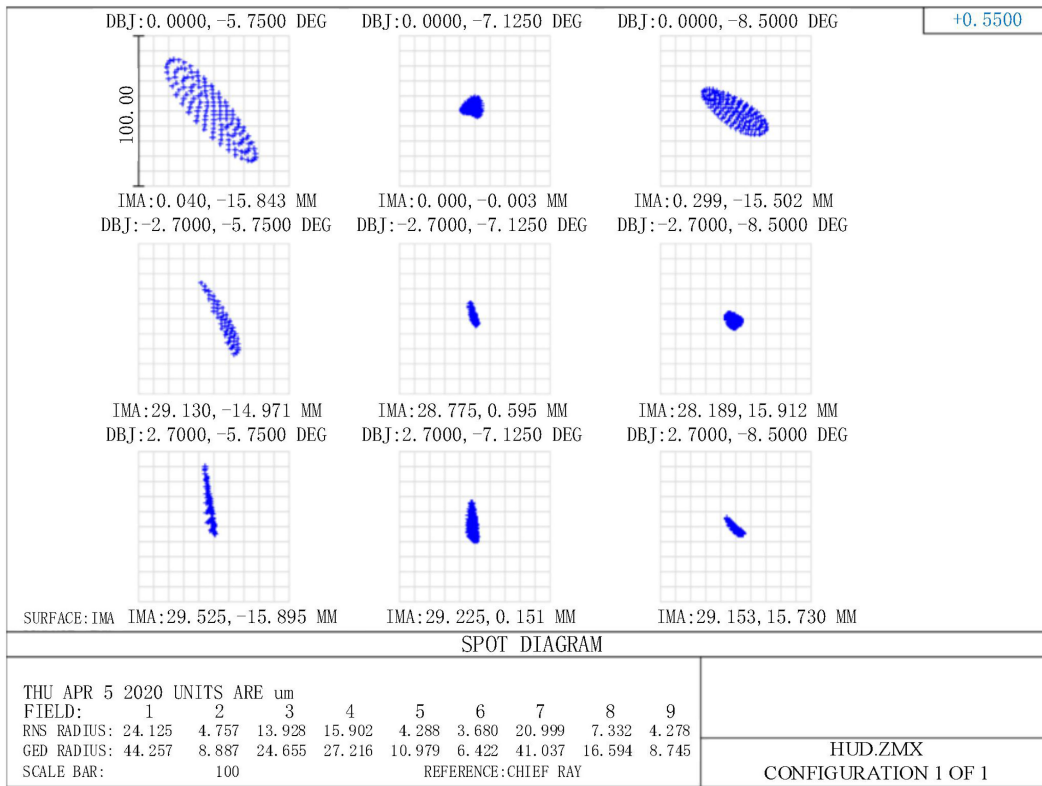


Fig. 6. Spot chart for the AR-HUD system.

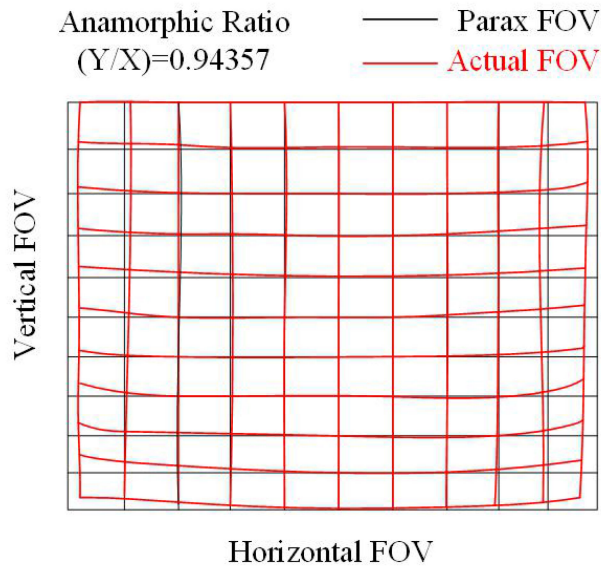


Fig. 7. Distortion curve of the system.



Fig. 8. Virtual reality fusion image of AR-HUD system.

TABLE 2  
Comparison of Different AR-HUD Systems

	Combiner AR-HUD	Windshield reflection type	New method
Principle			
Distance/m	1~1.5	2~2.5	2.8
Size of virtual image	3~8	9~10	11
Eye Box	130*50	130*50	140*60
Distortion	Under 4.5%	Under 5%	4%

we photographed the displayed results with the camera in the human eye. The result of the virtual reality fusion is shown in Fig. 8. The green arrow in the figure is the display image (virtual information) projected by the AR-HUD display. Table 2 shows a comparison between the system designed in this paper and conventional systems. Considering Table 2, we can see that the new AR-HUD system performs better than conventional systems. It not only improves security but also performs better.

### 3.2 AR-HUD System Registration Error

The experiments are carried out on 600 consecutive video images. The real coordinates of the feature points of the test image are taken as the benchmark. Then the estimated registration matrix is reprojected to obtain the reprojection coordinates of the registration matrix. By comparing

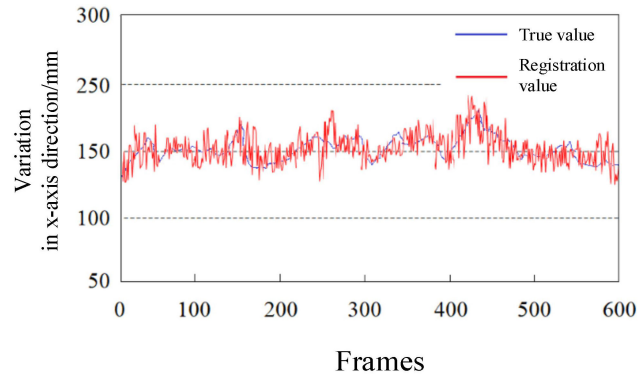


Fig. 9. Registration error in x-axis direction.

the reprojection coordinates with the real coordinates of feature points, the registration errors are obtained. Taking the translation component of the registration matrix in the x-axis direction as an example, the comparison results between the registered value and the real value are obtained. Fig. 9 shows the variation of each frame. In order to measure the similarity between the registered value and the real value, the error is evaluated by using the correlation distance.

After calculation, the correlation distance between the two groups of data is less than 0.1. Therefore, the two sets of data are highly similar, which means that the error is within the allowable range and meets the requirements of registration accuracy.

### 3.3 Safety Performance Evaluation of AR-HUD System

In the process of driving, the driver's attention is usually required to be highly concentrated. In complex road scenes, such as traffic congestion, sharp turns or low road visibility, the number of objects observed by the driver is limited. Results in the inability to pay attention to all objects in the scene. In this condition, the necessary information is reminded in front of the driver's vision to describe the road condition. This can improve driving safety to a certain extent. In addition, the vehicle information is usually concentrated on the instrument panel and navigation display. The driver frequently shifts his sight between the instrument panel and the road, and needs to move his head downward to get information. This information prompt mode is usually called head down display (HDD). Obviously, this way will increase the extra time, and in the long driving state, with the continuous change of visual focus, it will lead to driving fatigue. The AR-HUD system provides the necessary information in front of the driver's line of sight to improve the driver's spatial perception and reduce the response time in case of accidents. In order to further evaluate the performance of AR-HUD system, the response time and safety performance of the system are evaluated. The prompt information produced by AR-HUD has two functions, one can be used as visual enhancement function, and the other can be used as visual warning function. If the distance between an object and the vehicle is  $d$ , the speed of the vehicle is  $v_1$ , the moving speed of the object is  $v_2$ , and the speed of the object at rest is zero. The response time  $t$  of the driver to the object can be calculated by the following formula:

$$t = \left| \frac{d}{v_1 - v_2} \right| \quad (13)$$

The results of figure 10 show that at the same driving speed, the response time left by the HDD information prompt mode is less, while the AR-HUD system can reserve more response time for the driver. Similarly, in Fig. 11, with the increase of object distance, AR-HUD system reserves more reaction time for drivers than HDD, thus avoiding accidents.



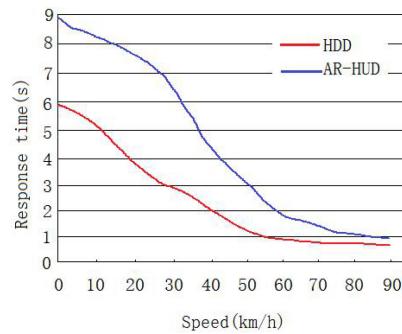


Fig. 10. Comparison of response time and speed in different ways.

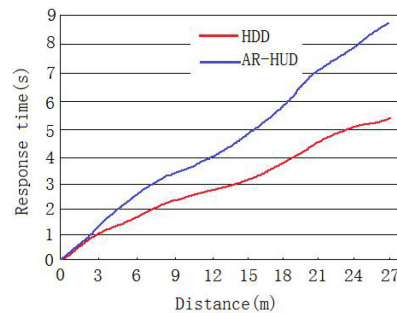


Fig. 11. Comparison of response time and distance in different ways.

The display effect of AR-HUD display is easily affected by the ambient light. The scene observed by the human eye is a mixture of the light from the real scene (for example, the light reflected from the road scene) and the color light of the augmented reality graphics. In car based augmented reality applications, the issue of color mixing is challenging because lighting conditions vary greatly from day to night driving in bright sunlight. Therefore, in the case of daytime driving, high-power LED array is used for lighting to ensure the brightness. When driving at night, adjust the lighting brightness and lower the brightness to avoid dizziness caused by long-time observation at night.

After ensuring the illumination brightness, another key problem of AR-HUD system is that changing the color of the display image will affect the contrast between the virtual image and the real world, thus affecting the contrast sensitivity and visual sensitivity. Visual acuity refers to the ability to see subtle details and is highly dependent on contrast. The driver's ability to recognize objects or distinguish virtual images is related to contrast, so the ability of drivers to quickly perceive and recognize virtual images is a function of image size and contrast. The relationship between size and contrast can be checked by changing the size and contrast. Virtual images are easily affected by contrast sensitivity, and the required contrast of graphic elements depends on the spatial frequency of graphics and the contrast between graphic elements and real background. Therefore, the contrast curve is studied in system, and the relationship between contrast and spatial frequency is shown in Fig. 12.

In the design of automotive augmented reality applications, it is important that users can see the shapes of objects of different sizes (cars, trucks, etc.) with different details and spatial frequencies. Therefore, in the driving scene, it is necessary to realize whether all objects of different sizes are normally visible under the same contrast and are just above the threshold value, or whether objects of different sizes need different contrasts to be visible normally. Through the above research, the AR-HUD prototype system is constructed and applied in the process of driving assistance to improve the driving safety.



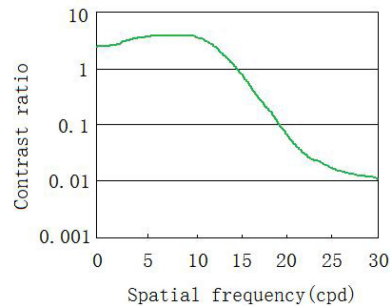


Fig. 12. Spatial frequency and contrast curve.

#### 4. Conclusion

This paper describes a novel AR-HUD system that can combine screen data with real-life information to increase the safety of a driver in a vehicle. The differences between off-axis reflective optical systems are analyzed, and a free-form surface was designed to serve as asymmetric aberration corrector. The optical system was designed for a virtual distance of 2.8m. The distortion near the center field of view is below 2%, the maximum distortion at the edge of the field of view is below 4%, and the MTF is greater than 0.4 at 6lp/mm. These numbers meet the required system specifications. In addition, we derived a relationship between the human eye, virtual image of optical system, and the real-life environment. After obtaining the environmental information, the virtual image is integrated into the real-life environment. Compared with conventional HUD systems, the new system performs better and driving safety can be improved.

#### References

- [1] C. Santos *et al.*, "Hybrid approach using sensors, GPS and vision based tracking to improve the registration in mobile augmented reality applications," *Int. J. Multimedia Ubiquitous Eng.*, vol. 12, no. 4, pp. 117–130, 2017.
- [2] V. Ng-Thow-Hing *et al.*, "User-centered perspectives for automotive augmented reality," in *Proc. Int. Symp. Mixed Augmented Reality - Arts, Media, Humanities IEEE*, 2013, pp. 13–22.
- [3] F. Liu and S. Seipel, "Precision study on augmented reality-based visual guidance for facility management tasks," *Automat. Construction*, vol. 90, no. 6, pp. 79–90, 2018.
- [4] G. Zhang, H. S. Chen, and Y. D. Ye, "A LoG operator based markerless augmented reality algorithm: LoG-PTAMM," *J. Comput.-Aided Des. Comput. Graph.*, vol. 28, no. 09, pp. 1577–1586, 2016.
- [5] B. Kress and T. Starner, "A review of head-mounted displays (HMD) technologies and applications for consumer electronics," in *SPIE Defense, Security, and Sensing*. Bellingham, WA, USA: International Society for Optics and Photonics, 2013.
- [6] J. W. Lee *et al.*, "A study of issues and considerations for development of a vehicle AR system," in *Proc. IEEE Int. Conf. Inf. Commun. Technol. Convergence*, 2015, pp. 1160–1162.
- [7] J. H. Lin *et al.*, "Design and implement augmented reality for supporting driving visual guidance," in *Proc. IEEE 2nd Int. Conf. Innovations Bio-Inspired Comput. Appl.*, 2012, pp. 316–319.
- [8] P. R. J. A. Alves *et al.*, "Forward collision warning syst. using heads-up displays: Testing usability two new metaphors," in *Proc. IEEE Intell. Veh. Symp.*, 2013, pp. 1–6.
- [9] Z. C. Cao and L. Dai, "Application of HUD on automobile and domestic and international developments," *Chin. Building Mater. Sci. Technol. J.*, vol. S2, no. 10, pp. 16–18, 2010.
- [10] F. Yang, S. H. Lin, and C. J. Wu, "Application of head up display system in automobile," *Light Veh.*, vol. Z4, no. 12, pp. 24–26+16, 2013.
- [11] T. Poitschke *et al.*, "Contact-analog information representation in an automotive head-up display," in *Proc. Symp. Eye Tracking Res. Appl. ACM*, 2008, pp. 119–122.
- [12] L. Pfannmüller *et al.*, "A comparison of display concepts for a navigation system in an automotive contact analog Head-up display," *Procedia Manuf.*, vol. 3, no. 1, pp. 2722–2729, 2015.
- [13] H. Karvonen, T. Kujala, and P. Saariluoma, "In-car ubiquitous computing: Driver tutoring messages presented on a head-up display," in *Proc. IEEE Intell. Transp. Syst. Conf.*, 2006, pp. 560–565.
- [14] M. Tonnis, C. Lange, and G. Klinker, "Visual longitudinal and lateral driving assistance in the head-up display of cars," in *Proc. IEEE ACM Int. Symp. Mixed Augmented Reality*, 2008, pp. 91–94.
- [15] Y. Ohe *et al.*, "Application of a novel photopolymer to a holographic head-up display," *Polymers Adv. Technol.*, vol. 10, no. 9, pp. 544–553, 2015.

- [16] H. Peng *et al.*, "Design and fabrication of a holographic head-up display with asymmetric field of view," *Appl. Opt.*, vol. 53, no. 29, pp. 177–185, 2014.
- [17] E. Buckley and D. Stindt, "Full colour holographic laser projector HUD," *Buckley Full CH*, vol. 1, no. 1, pp. 1–5, 2008.
- [18] F. Guo and J. Zhao, "Diffraction characteristics of HUD holographic combiner," *Acta Photonica Sinica*, vol. 3, no. 3, pp. 350–352, 2004.
- [19] K. Bang *et al.*, "Curved holographic optical elements and applications for curved see-through displays," *J. Inf. Display*, vol. 20, no. 1, pp. 9–23, 2019.
- [20] M. Moleron, M. Serra-Garcia, and C. Daraio, "Acoustic fresnel lenses with extraordinary transmission," *Appl. Phys. Lett.*, vol. 105, no. 11, 2014, Art. no. 104103.
- [21] A. Davis, "Fresnel lens solar concentrator derivations and simulations," *Proc. SPIE - Int. Soc. for Opt. Eng.*, vol. 8129, no. 7, pp. 153–159, 2011.
- [22] T. Tsaliev and Z. Veliev, "Cylindrical fresnel lenses," in *Proc. IEEE Int. Conf. Math. Methods Electromagn. Theory*, 2008, pp. 395–397.
- [23] Y. Wang, L. Jiang, and S. Zhihua, "Optical design of ensemble head-up display system based on mini-projector," *Laser Optoelectron. Prog.*, vol. 55, no. 11, pp. 424–430, 2018.
- [24] Z. Xiaofeng *et al.*, "Research on brightness perception model based on night vision vehicle head up display," *Laser Optoelectron. Prog.*, vol. 54, no. 12, 2017, Art. no. 121501.
- [25] C. Fang, C. Xiaoqiang, and L. Shenghui, "Design of HUD mini-projector display optical system based on DLP," *Opt. Optoelectronic Technol.*, vol. 15, no. 1, pp. 86–89, 2017.
- [26] L. Gu *et al.*, "Design and fabrication of an off-axis four-mirror system for head-up displays," *Appl. Opt.*, vol. 59, no. 16, pp. 4893–4990, 2020.
- [27] K.-H. Kim *et al.*, "Design of confocal off-axis two-mirror system for head-up display," *Appl. Opt.*, vol. 58, no. 3, pp. 677–683, 2019.
- [28] Z. Qin *et al.*, "Dual-focal-plane augmented reality head-up display using a single picture generation unit and a single freeform mirror," *Appl. Opt.*, vol. 58, no. 20, pp. 5366–5374, 2019.
- [29] B.-H. Kim and S.-C. Park, "Optical system design for a Head-up display using aberration analysis of an off-axis two-mirror system," *J. Opt. Soc. Korea*, vol. 20, no. 4, pp. 481–487, 2016.
- [30] S. Wei *et al.*, "Design of a head-up display based on freeform reflective systems for automotive applications," *Appl. Opt.*, vol. 58, no. 7, pp. 1675–1681, 2019.
- [31] L. Xu, H. T. Zhao, and S. Y. Sun, "Monocular infrared image depth estimation based on deep convolutional neural networks," *Acta Optica Sinica*, vol. 36, no. 7, pp. 196–205, 2016.
- [32] P. J. Besl and N. D. McKay, "A method for registration of 3-D shapes," *IEEE Trans. Pattern Anal. Mach. Intell.*, vol. 14, no. 2, pp. 239–256, Feb. 1992.